## **Architectural Dimensions and Beyond**



www.adb.reapress.com

Arch. Dim. Bey. Vol. 2, No. 4 (2025) 257-276.

Paper Type: Original Article

# Earthquake-Resistant Architectural Design Using a Hybrid Neural Network Approach for Optimizing **ADAS Dampers in Steel Buildings**

Saman Rahimi<sup>1</sup>, Amirhossein Fazeli<sup>1,\*</sup>

<sup>1</sup> Department of Civil Engineering, Deakin University, WaurnPonds, Geelong, Australia; Samanr.r.ac@gmail.com, Nejati@aihe.ac.ir. Citation:

> Received: 29 December 2024 Revised: 15 March 2025 Accepted: 10 May 2025

Rahimi, S., & Fazeli, A. (2025). Earthquake-resistant architectural design using a hybrid neural network approach for optimizing ADAS dampers in steel buildings. Architectural dimensions and beyond, 2(4), 257-276.

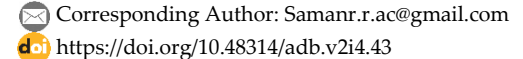
#### **Abstract**

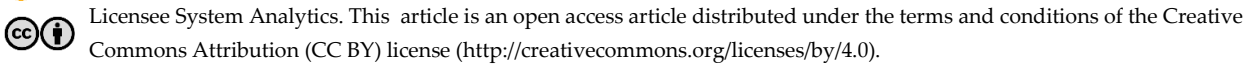
Earthquake-resistant architectural design is a key approach to improving the safety and sustainability of high-rise buildings. The use of modern technologies, such as artificial intelligence and energy dissipation devices, enables the simultaneous enhancement of structural performance and architectural design quality. In this study, a hybrid method based on Artificial Neural Networks (ANNs) is proposed to optimize the performance of Added Damping And Stiffness (ADAS) dampers in steel buildings. To evaluate the effectiveness of this approach, a 15-story steel structure with a braced system was modeled in four different retrofit configurations and analyzed using nonlinear Incremental Dynamic Analysis (IDA) with 10 earthquake acceleration records. The initial design was conducted in ETABS, while the analysis and optimization were performed in OpenSees and MATLAB. The results indicate that the application of ADAS dampers increases stiffness, reduces inter-story drifts, and improves the overall seismic behavior of the building. Ultimately, the study demonstrates that integrating intelligent methods into architectural and structural design can provide a practical pathway to developing earthquake-resistant, resilient architecture.

Keywords: Earthquake-resistant architecture, Added damping and stiffness damper, Artificial neural network, Seismic optimization, Steel building, Intelligent architectural design.

## 1 | Introduction

Since the dawn of human civilization, people have continually faced natural geological events and have tried to predict or control them to protect themselves from potential hazards. Among these natural disasters, earthquakes have undoubtedly been among the most destructive and damaging events throughout history, whether in times when humans primarily lived in villages or in the present era, when the majority reside in cities and metropolitan areas. Iran, in particular, is one of the most seismically active regions in the world and has consistently faced diverse, and sometimes catastrophic, natural hazards, a trend expected to continue.





From a tectonic perspective, the Iranian crust lies at the collision zone of tectonic plates, making the region highly susceptible to various types of earthquakes. Unfortunately, most of the country's major cities, including the capital, are located in areas of high or very high seismic risk, often near active faults. In addition, increasing population density in metropolitan areas has, from an engineering standpoint, amplified the potential for casualties and structural damage during earthquakes, floods, and other disasters.

One of the significant challenges worldwide is the damage caused by natural hazards such as earthquakes, storms, and fires. Iran's geographic and environmental conditions make it among the most vulnerable regions on Earth, particularly with respect to earthquakes. Historically, these events have caused significant economic losses. According to global rankings of countries by the frequency of hazardous earthquakes from 1990 to 2016, Iran is the third-most earthquake-prone country in the world, after China and Indonesia. The country is situated at the convergence of the Eurasian and Arabian tectonic plates, making earthquakes inevitable. Since the exact time and location of earthquakes cannot be predicted, one of the primary concerns in earthquake and structural engineering is finding effective methods to control and mitigate seismic damage.

Structural control systems are generally classified into three categories: passive, active, and semi-active control. Added Damping And Stiffness (ADAS) dampers are among the oldest energy dissipation devices used to reduce the seismic response of structures during strong earthquakes.

In this study, we aim to determine the optimal design parameters of ADAS dampers in a steel structure using a hybrid neural network approach, thereby maximizing the damper's efficiency in energy dissipation and structural control. Currently, based on recent research, fixed values are often used for the design parameters of ADAS dampers. To address this issue, nonlinear analysis software is employed for optimization, while SAP2000 is used for structural modeling and nonlinear analysis.

Given the importance of structural optimization, researchers in recent years have been seeking innovative methods to solve optimization problems, aiming to replace conventional mathematically-based techniques with advanced approaches. Accordingly, in this study, a hybrid neural network method is applied to determine optimal ADAS damper design parameters with higher accuracy and efficiency than traditional analytical methods.

## 2 | Literature Review

Over the years, numerous studies have addressed reducing the seismic response of structures under dynamic loads. One of the primary methods for mitigating such responses is the use of passive control systems, which utilize various types of dampers to absorb and dissipate a portion of the input seismic energy. In passive systems, damping is produced without the need for an external energy source [1].

Over the past few decades, several innovative concepts for developing energy-dissipation devices have been proposed. The idea of using yielding steel plates to improve the seismic performance of structures was first introduced in the 1970s for a nuclear power plant in the United States, and since then, significant advancements have been made in this field [2]. These dampers utilize the plastic deformation (hysteretic) behavior of metals to dissipate energy, thereby enhancing both energy dissipation capacity and structural system stiffness.

Research conducted by Tehrani-Zadeh [3] at Amirkabir University investigated the effect of yielding dampers on the seismic response of Moment-Resisting Steel Frames (MRSFs) with bracket-type connections [4]. To overcome certain shortcomings and improve the stability of yielding metallic dampers, newer studies introduced alternative damper geometries. In these studies, triangular-shaped elements replaced the conventional X-shaped plates, and slotted openings were provided to allow vertical flexibility of the plates [5]. Experimental results showed that ADAS dampers equipped with triangular (T-ADAS) plates exhibited distinct improvements in mechanical characteristics. The triangular geometry prevents premature buckling under axial forces, ensuring greater stability and higher energy dissipation efficiency [6].

In 1992, Xia and Hanson [6] conducted a comprehensive study of the influence of design parameters on the seismic behavior of moment-resisting frames equipped with ADAS dampers. Their work produced positive results and proposed specific values for key design parameters [7], drawing on the analytical models developed by Workman and Akkar [8], [9].

Early studies on performance-based seismic design, such as those by Moghaddam [10] and colleagues, demonstrated that multiple acceptable design solutions can achieve the same target performance level, but these solutions are not necessarily identical. Subsequent nonlinear dynamic analyses confirmed that conventional seismic design methods do not lead to a uniform distribution of ductility across a structure [11]. Similarly, Karami's studies revealed that by properly controlling the strength distribution within a structure, the maximum ductility demand under strong earthquakes can be significantly reduced.

These findings collectively indicate the growing importance of developing optimized and adaptive damper design approaches, especially for modern steel structures, where achieving a balance between architectural integrity and structural performance is essential. A broader perspective emerging from these studies is that the arrangement and distribution of a structure's properties can be designed so that, with a fixed amount of material and construction cost, the structure achieves superior seismic performance during destructive earthquakes. Therefore, an optimal solution refers to a configuration that provides the best performance among all possible alternatives under specific conditions [12].

In 2019, Nabid et al. [13] conducted a study aimed at improving computational efficiency and convergence rate in the Uniform Deformation Optimization Method and evaluating its reliability compared to other heuristic optimization techniques such as the Genetic Algorithm (GA). To assess the effectiveness of the proposed approach, 3-, 5-, and 10-story frames equipped with friction dampers were optimized using the uniform deformation method, the GA, and a hybrid combination of both. The results demonstrated that the uniform deformation method could provide an optimal design solution with significantly lower computational cost—up to 300 times less than nonlinear dynamic analyses—compared to GA and hybrid approaches. Consequently, the uniform deformation optimization method was considered a reliable and efficient tool for the design of friction dampers [14].

In 2018, researchers at the Asian Institute of Technology (AIT), Thailand, compared ADAS dampers with toothed (shear-type) dampers in terms of material type and plate count. Their findings revealed that the steel ADAS damper with fewer plates exhibited superior performance and higher efficiency [15].

In another study, Yang et al. [16] conducted experimental investigations on steel shear walls under shear, compression, and cyclic seismic loading. Their results strongly recommended that the shear capacity and stiffness of steel shear walls be reduced by a modification factor that primarily depends on the depth-to-thickness ratio of the steel plate and the magnitude of the applied gravity load [17].

More recently, Domenico and Ricciardi [18] examined the seismic protection of existing structures with limited seismic capacity using yield-type dampers subjected to torsional oscillations. Many essential facilities, such as hospitals, fire stations, schools, and power plants, do not comply with modern seismic codes because they were designed to outdated construction standards. Given the critical importance of these structures, maintaining their stability and structural integrity during and after an earthquake is paramount. Therefore, the use of seismic isolation and damping systems has become increasingly widespread. In their research, two retrofitting strategies were compared: 1) base isolation systems equipped with mechanical mechanisms, and 2) hybrid systems combining base isolation with yielding-type dampers. Their findings confirmed the effectiveness of the latter approach in enhancing seismic resilience [19].

Peruš and Fajfar, investigated the optimization of a steel-yielding linear damper for multistory buildings. In this study, the structure was modeled using an inner-spring damping configuration for a multistory building, with an ADAS-type damper. The damper's base stiffness was also considered in the analysis. Four optimal damper configurations were determined to minimize the maximum inter-story drift of the structure, accounting for the effects of moment magnitude and base stiffness [20].

Also, in 2023, Shojaeifar et al. [15] examined the performance of Triangular Yielding Metallic Dampers (TADAS) and curved-element dampers installed in MRSFs. These passive dampers were positioned at the beam-to-column connections. The study's variable parameters included the thickness of the curved elements (50, 75, and 100 mm), the thickness of the triangular dampers (5 and 10 mm), and the number of dampers (2, 4, and 6). The evaluations were performed using the Finite Element Method (FEM) in ABAQUS software. Two experimental studies were conducted to validate the numerical simulation approach, showing strong agreement. The frame responses under different configurations were compared in terms of energy dissipation, strength, residual damping ratio, and ductility. The comparison revealed that dampers equipped with curved elements effectively reduced the structural responses to seismic loading, dissipated a significant amount of input seismic energy, and consequently prevented permanent structural damage. The behavior of this damper system demonstrated that, through controlled deformation, a large portion of seismic energy can be efficiently absorbed and dissipated [21].

In 2024, Khoshkalam et al. [17] reviewed various types of yielding dampers with different configurations and elements developed to improve the seismic performance of structures. For ADAS dampers, which dissipate energy based on their geometric configuration, it is expected that, under severe earthquakes, they exhibit uniform, controlled yielding behavior. The study revealed that X-shaped dampers cannot maintain optimal performance under large deformations when subjected to unexpected axial tensile forces. The axial force not only causes localized strain in the middle of the X-shaped plates but also increases the stress level on the damper, potentially damaging its main components. To overcome these issues, the paper proposed a Modified ADAS Damper (MADAS) with a geometry similar to that of conventional ADAS and boundary conditions similar to those of TADAS. In the proposed configuration, the axial force is transferred to the braces through side plates rather than triangular ones, thereby improving overall performance. To design an optimal damper, an analytical equation for determining the maximum shear stress was developed using ABAQUS modeling and a detailed parametric study. Results showed that in the nonlinear range, the MADAS damper's force level is approximately 30% higher than that of the conventional ADAS model, indicating a significant improvement in energy dissipation capacity and overall efficiency. For conventional ADAS dampers, the force level increases by more than 150%, whereas for the MADAS damper, it remains significantly lower. Moreover, the maximum equivalent plastic strain observed in the ADAS model was found to be twice that of the MADAS configuration. In addition, evaluations of monotonic, cyclic, and dynamic behaviors revealed that the newly proposed MADAS dampers demonstrate substantial energy dissipation capacity under large deformations. These results confirm the improved stability, efficiency, and seismic performance of the modified damper design [22].

## 3 | Modeling and Research Methodology

In the literature review phase, existing sources were used to define and introduce the study's key concepts and keywords. In the field study phase, the focus was on modeling and analyzing structural behavior. The selected building plans were intentionally asymmetric to account for torsion effects on structural response. A 15-story steel structure with braced frames was modeled and analyzed under four different retrofitting configurations using ADAS dampers placed in various bays, representing four distinct damper layouts. The selection criterion for this model was to evaluate the seismic behavior of high-rise structures and to determine the optimal damper arrangement for improved seismic performance. For this purpose, Incremental Dynamic Analysis (IDA) was performed using at least ten near-fault ground motion records, each with an epicentral distance of less than 15 kilometers, as recommended by FEMA-P695. This selection ensures that the applied earthquake records are both reliable and critical for seismic assessment. The initial design of the structures was conducted using ETABS, while nonlinear dynamic analyses were performed using OpenSees to evaluate and optimize the seismic performance of the damped structural models.

#### 3.1 | Artificial Neural Networks

Artificial Neural Networks (ANNs) are linear or nonlinear mapping systems between two specific spaces. Once the network is trained or adjusted, a particular input produces a corresponding output. As illustrated in the figure below, the training process continues until the network output matches the desired output (commonly called the target). The network adapts based on the comparison between the input and the target.

In the field of civil engineering, ANNs have been successfully applied to various areas, including structural analysis and design, damage detection, and structural control. ANNs are considered practical regression tools because they exhibit strong nonlinearity and can model complex relationships between input and output variables without prior knowledge of the underlying problem.

In this research, a multilayer neural network with the Back-Propagation (BP) learning algorithm is used to estimate the optimal design parameters of the ADAS damper subjected to successive critical earthquake records. The BP network is a multilayer structure employing nonlinear transfer functions and the Widrow–Hoff learning rule. Using input and target vectors, the network learns to approximate a function, identify the relationship between inputs and outputs, and classify the input data.

This network, which includes a bias term, one or more hidden sigmoid layers, and a linear output layer, can approximate any function with a limited number of discontinuities. The standard BP algorithm is a gradient-descent-based method in which the network weights are updated in the direction opposite to the gradient of the performance function. Initially, the weights are randomly assigned; at each step, the network computes its output, and based on the difference between the actual and target outputs, the weights are iteratively adjusted to minimize the error.

In this algorithm, each neuron's activation function is defined as the weighted sum of its input signals. To establish a more efficient connection between the error and the network parameters (inputs, weights, and outputs), the Levenberg–Marquardt (LM) optimization algorithm is utilized. This method, which combines the Newton–Gauss and steepest descent methods, is a standard approach for nonlinear least-squares problems. The algorithm randomly divides the available dataset into three subsets — training, validation, and testing — to ensure robust generalization of the model.

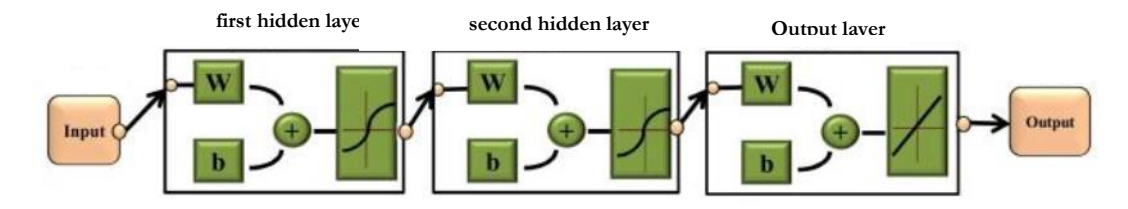


Fig. 1. Schematic representation of the neural network architecture used in this study.

In the present study, 60% of the available data were used for training, 35% for testing to prevent overfitting, and the remaining 5% for neural network validation. The Mean Squared Error (MSE) was used as the training stopping criterion, with lower MSE values indicating better network performance and an MSE of zero indicating a perfect fit with no error.

Additionally, the regression coefficient (R) was used to represent the degree of correlation between the network outputs and the target values. An R value of 1.0 indicates perfect correlation, while R=0 implies an entirely random and uncorrelated relationship. Hence, both MSE and R were considered as key performance indicators for selecting the optimal neural network model.

To achieve a reliable neural network model, it is crucial to use homogeneous and consistent input data. Accordingly, several parameters related to earthquake characteristics—including Peak Ground Acceleration (PGA), Effective Peak Acceleration (EPA), and the first and second seismic magnitudes—along with structural parameters such as building type and height, were incorporated into the model through the structural period (T). The reduced response factor obtained from successive earthquake scenarios, along with

the results of the frame analyses performed in this study, were used as target values for training, testing, and validation. In this context, the period parameter (T) is the key factor distinguishing the results across the analyzed frames.

To avoid overfitting, the number of hidden-layer neurons was carefully chosen. This parameter significantly influences network performance: a hidden layer that is too small may fail to capture the data's complexity. At the same time, one that is too large can lead to overfitting, resulting in high-frequency oscillations and poor generalization.

As previously mentioned, the sigmoid transfer function was used in the network's hidden layers, which operate within the range 0 to 1. Therefore, before training, all data—both inputs and targets—were normalized. A linear interpolation method was adopted for data scaling to ensure uniform data distribution. After introducing the normalized input and target datasets into the network and performing training until the error was minimized, the final optimized outputs were obtained.

#### 3.2 | Material Properties

The structural system under investigation is steel-framed. In modeling the structure's linear behavior, lower-bound material properties were adopted to ensure safety and conservatism within the elastic range. Conversely, in modeling the nonlinear behavior of deformation-controlled elements, the expected material strengths were used in accordance with the provisions of FEMA-356 and the Seismic Rehabilitation Guidelines.

$$Fy := \cdot 2400 \cdot \frac{kg}{cm^2},$$

$$Fu := 3700 \cdot \frac{kg}{cm^2}$$

Fye :=: 
$$1.1(2400) :=: 2640 \cdot \frac{\text{kg}}{\text{cm}^2}$$

Fue 
$$\rightarrow$$
 1.1(3700)  $\rightarrow$  4070  $\cdot \frac{\text{kg}}{\text{cm}^2}$ .

#### 3.3 | Definition of Dead and Live Loads

In this stage, two types of loads—dead load and live load—are defined in the analysis program. Additionally, a lateral load pattern is applied in the direction of the nonlinear static (pushover) analysis, with the base shear coefficient calculated in accordance with Chapter 6 of the Iranian Building Code.

In this study, the dead load on all floors is assumed to be 500 kg/m², and the live load is taken as 250 kg/m². These values represent typical load distributions for steel structures and are applied uniformly across all stories.

#### 3.4 | Definition of Lateral Loads

The structural systems considered in this study are a 15-story steel building with braced frames, in accordance with *Table 1* of the Iranian Seismic Code.

Ts	$T_0$	S	$S_0$	A	
0.7	0.15	1.75	1.1	0.35	
$T=0.05*H^{0.9}$	В	N	$B_1 = (S+1)*(T_S/T)$	Ι	15 story building
1.54	1.57	1.26	1.25	1	15-story building
K=0.5T+0.75	C=ABI/R	$C_{d}$	$\Omega_0$	R	
1/52	0.07	5.5	3	7.5	

Table 1. Seismic coefficients for application in SAP software for the 15-story structure.

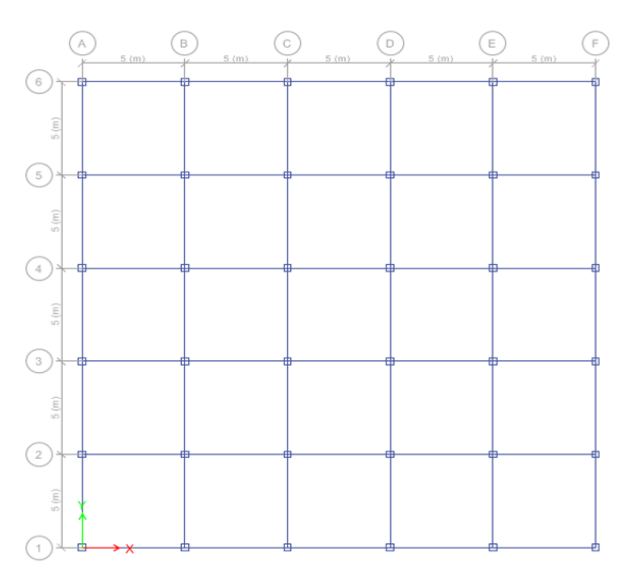


Fig. 2. Plan of the investigated structures.

15-Story Structure With a Concentric Braced Frame System				
<b>Brace Sections</b>	Column Sections	Beam Sections		

Table 2. Assigned sections for the structures modeled in ETABS.

	15-Story Structure With a Concentric Braced Frame System						
<b>Brace Sections</b>		Column Sections	Beam Sections				
	Tubo 140*140*14.2	Box 500*500*20	IPE 360	Brace sections			
	Tubo 140*140*14.2	Box 400*400*15	IPE 360	Floors 6 to 10			
	Tubo 140*140*14.2	Box 350*350*15	IPE 330	Floors 10 to 11			

## 4 | Design of the Structure with Dampers

Typically, the inherent damping of conventional structures is around 5%, and based on this damping, the design response spectra are initially plotted. However, when dampers are incorporated into the structure, the peak acceleration values of the spectrum are reduced.

At the beginning of the design process, there is usually no prior information about the damper. Therefore, when modeling a linear damper in SAP2000, it is necessary to define the damper properties, such as effective stiffness and effective damping, within the software. Consequently, nonlinear dampers are generally avoided, as conventional structural analysis software like SAP often encounters convergence issues with highly nonlinear elements.

In this study, linear dampers were employed. To ensure the damper behaves linearly, its stiffness must be sufficiently high, but not excessively high, to prevent convergence problems during analysis. It is recommended that the ratio.

 $\lambda = CDKD \setminus ambda = \int c(C_D KD) \lambda = KDCD.$ 

It is one order of magnitude smaller than the time step of the applied load ( $\Delta t$ ). For example, the damper stiffness can be selected according to the following guideline [6]:

$$K_D = \frac{100C_D}{\Delta t}$$

Where CDC\_DCD is the damping coefficient of the damper.

According to the NEHRP and ASCE 7-10 codes, the overall structural damping ratio is calculated using the following equation:

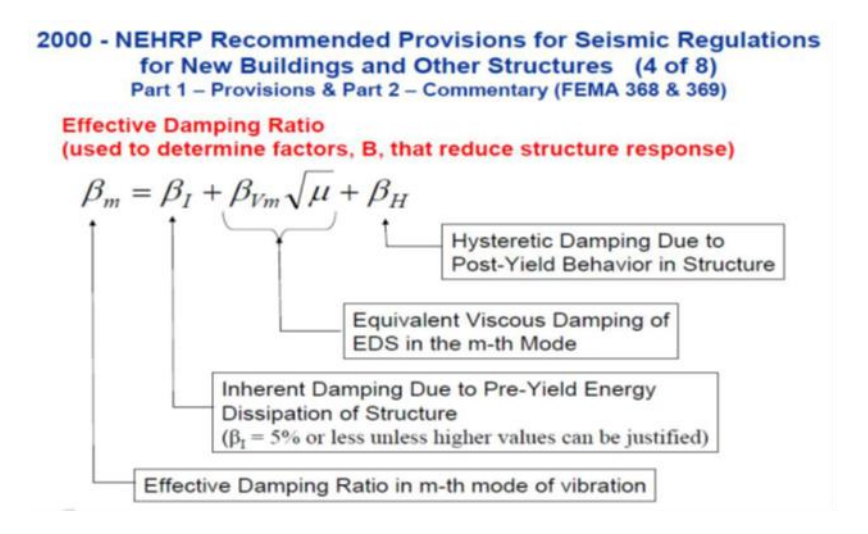


Fig. 3. Method for calculating the overall structural damping ratio.

All dampers used in the structure must comply with the relevant code provisions. Therefore, in this study, ADAS yielding dampers with the specifications listed in *Table 3* were employed. Each damper consists of several X-shaped elements (for ADAS dampers). The behavior of the dampers is modeled as bilinear with strain hardening.

Table 3. Mechanical properties of the metallic dampers (added damping and stiffness, triangular yielding metallic dampers) used in the models.

Figure	b (Cm)	h (CVm)	t (Cm)	K (Cm)	V <sub>y</sub> (kg)	$\Delta_{\rm y}({\rm cm})$
$\left\{\begin{array}{c} h \\ h \end{array}\right\}$	20	30	1.5	5625	1350	0.24

Table 4. Assigned sections for all investigated structures in SAP.

15-Story Structure With A Concentric Braced Frame System					
Brace sections	Column sections	Beam sections			
Tubo 140*140*14.2	Box 500*500*20	IPE 360	Floors 1 to 5		
Tubo 140*140*14.2	Box 400*400*15	IPE 360	Floors 6 to 10		
Tubo 140*140*14.2	Box 350*350*15	IPE 330	Floors 10 to 11		

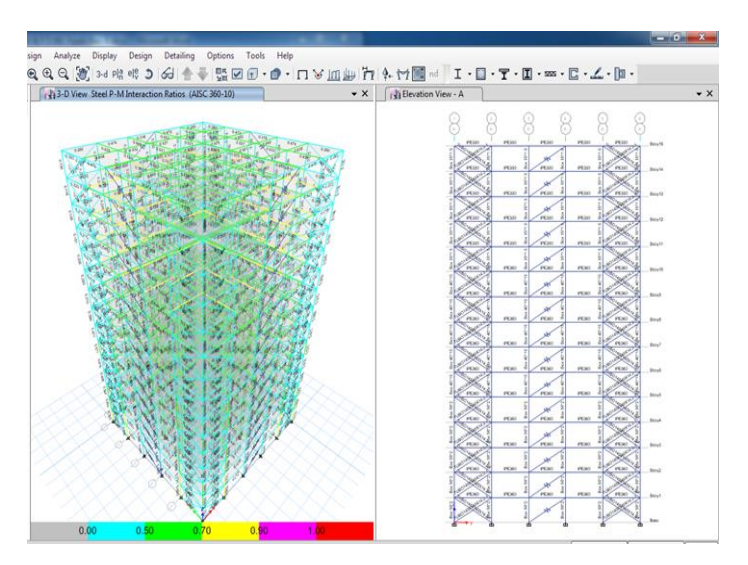


Fig. 4. Layout of the first damper configuration in the structures (TYPE 1).

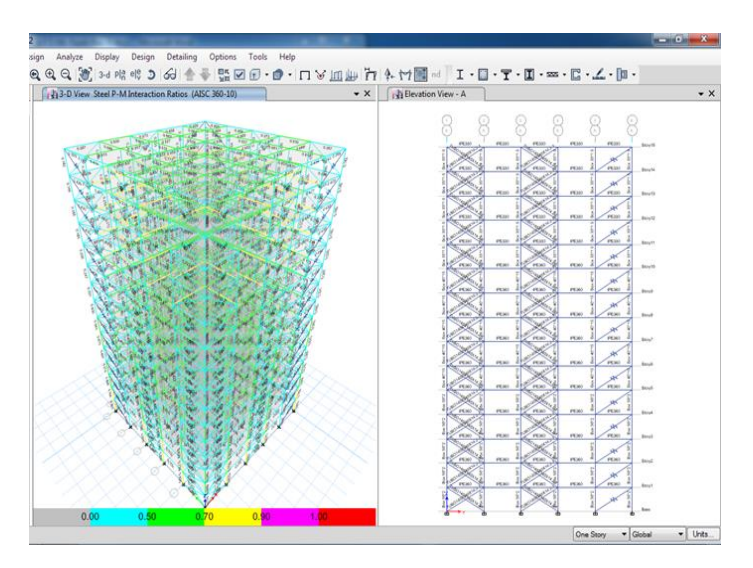


Fig. 5. Layout of the second damper configuration in the structures (TYPE 2).

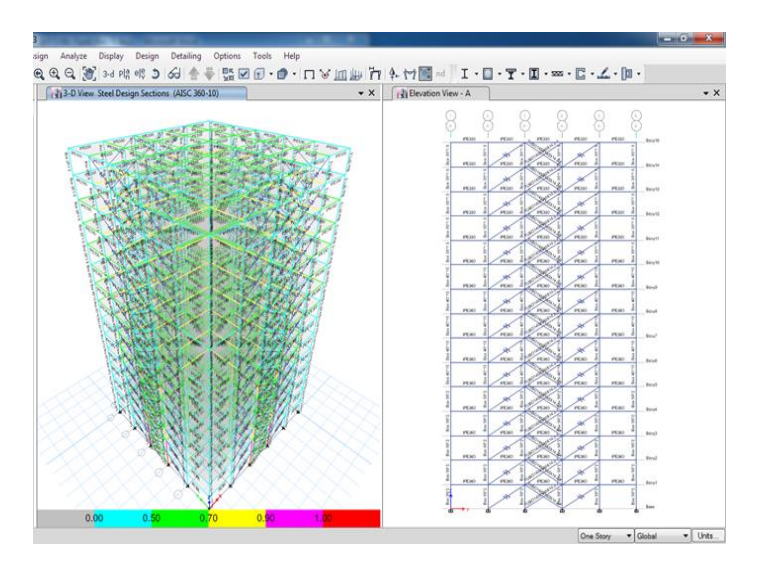


Fig. 6. Layout of the third damper configuration in the structures (TYPE 3).

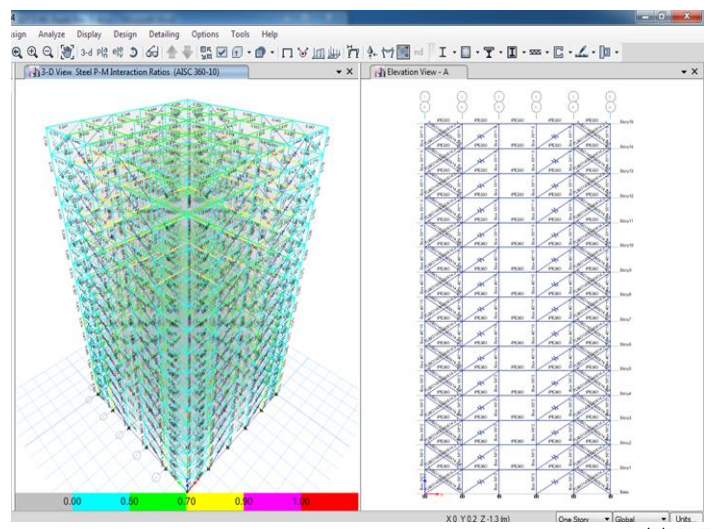


Fig. 7. Layout of the fourth damper configuration in the structures (TYPE 4).

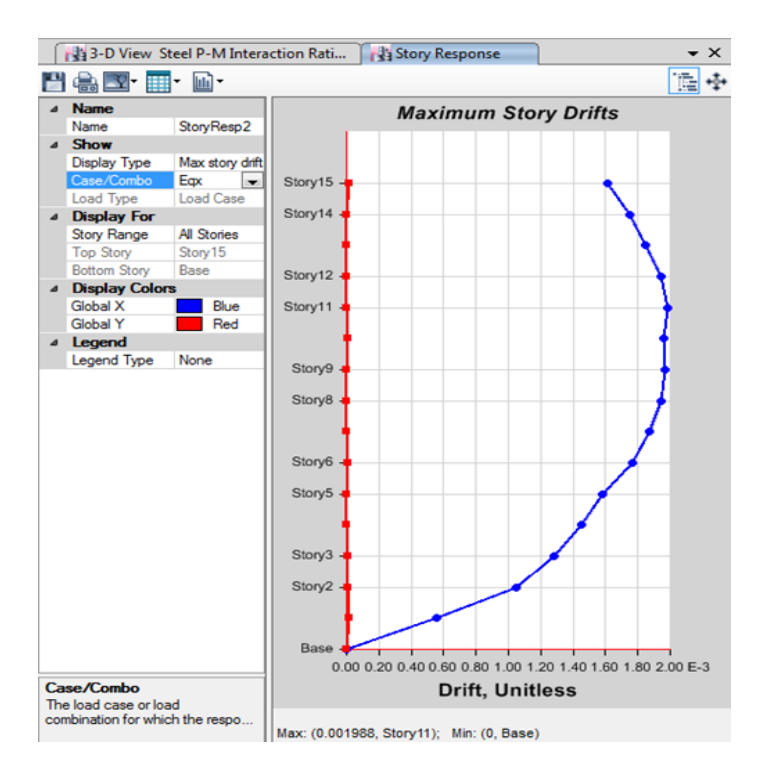


Fig. 8. General schematic of structural drift for configuration (TYPE 1).

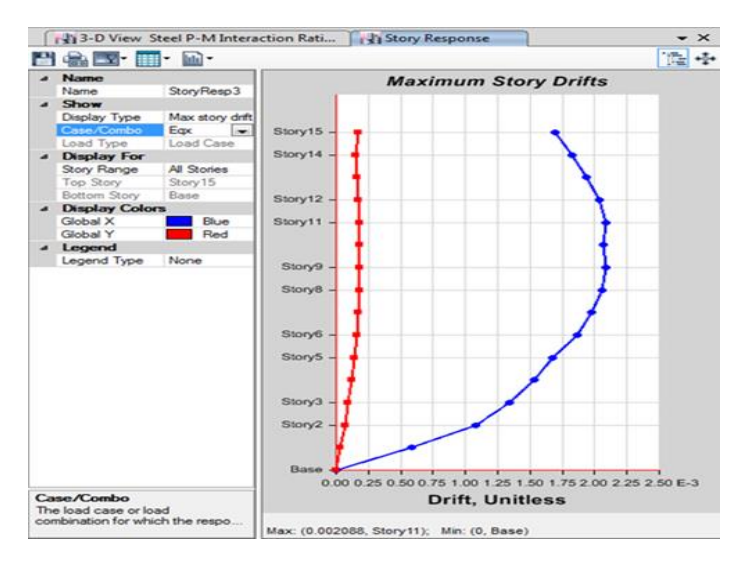


Fig. 9. General schematic of structural drift for configuration (TYPE 2).

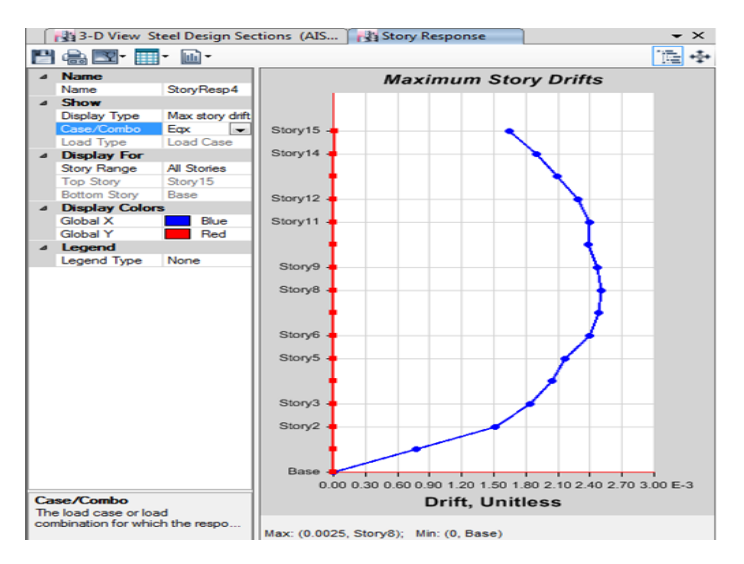


Fig. 10. General schematic of structural drift for configuration (TYPE 3).

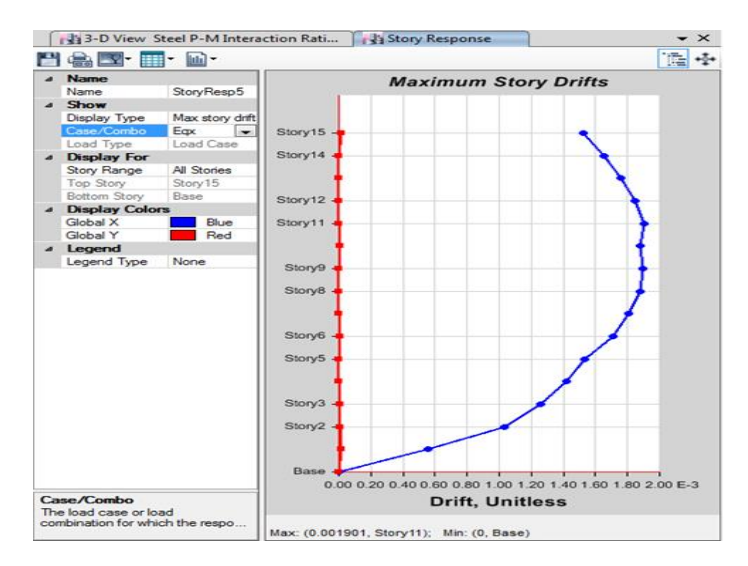


Fig. 11. General schematic of structural drift for configuration (TYPE 4).

#### 5 | Analysis and Interpretation of Results

#### 5.1 | Incremental Dynamic Analysis Results

The selected frames of the structures under investigation were modeled in OpenSees as two-dimensional frames, and a general schematic of the modeled frames is provided. The IDA results were obtained, and the 50% mean values for all three frames are shown in the figures below.

In this context, a neural network technique was employed using MATLAB and OpenSees to assist in the analysis and interpretation of the results.

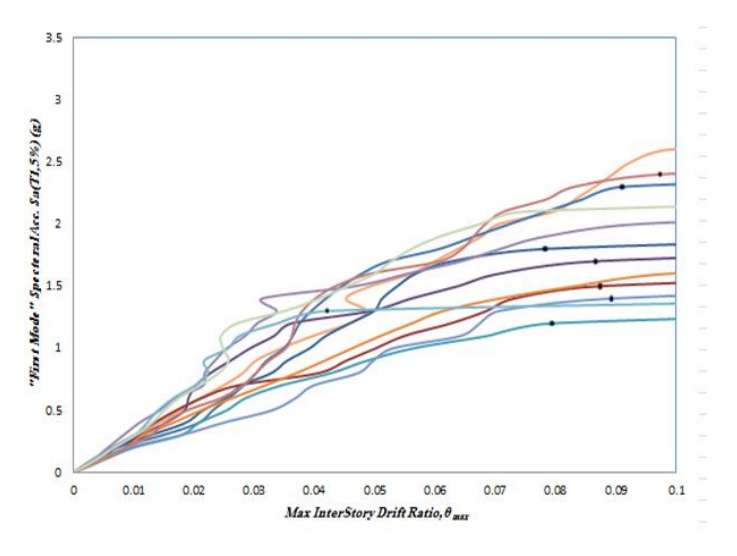


Fig. 12. Incremental nonlinear dynamic curves obtained for the 15-story structural frame (TYPE 1).

Fig. 12 presents the incremental nonlinear dynamic curves for the 15-story structural frame of TYPE 1. Additionally, in Fig. 13, a summary of the IDA curves is shown, representing the 16%, 50%, and 84%.

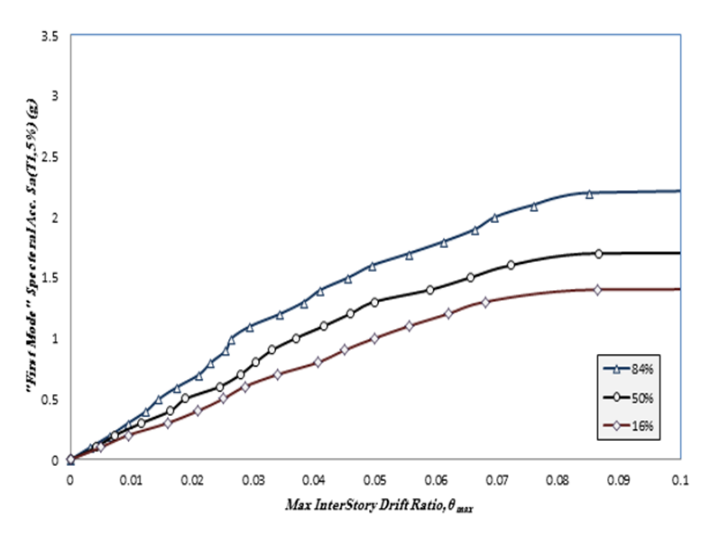


Fig. 13. 16%, 50%, and 84% percentile curves of the incremental nonlinear dynamic analysis for the 15-story structural frame (TYPE 1).

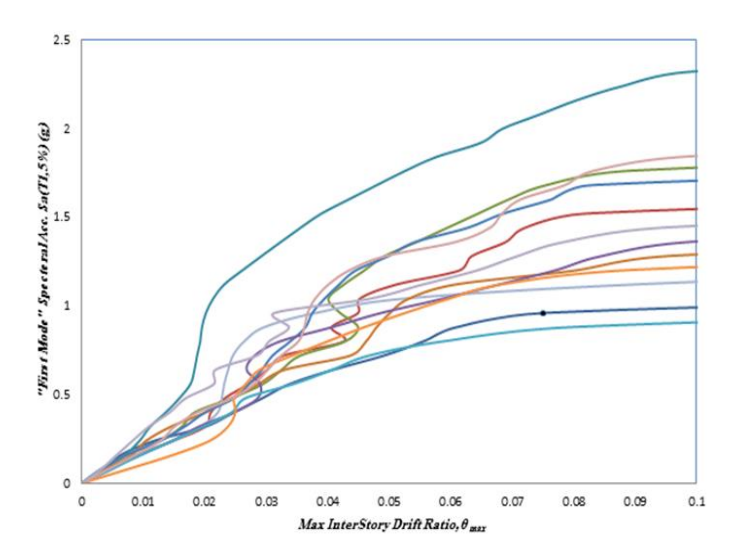


Fig. 14. Incremental nonlinear dynamic curves for the 15-story structural frame (TYPE 2).

Fig. 14 presents the incremental nonlinear dynamic curves for the 15-story structural frame of TYPE 2. Additionally, in Fig. 15, a summary of the IDA curves is shown, representing the 16%, 50%, and 84% percentiles.

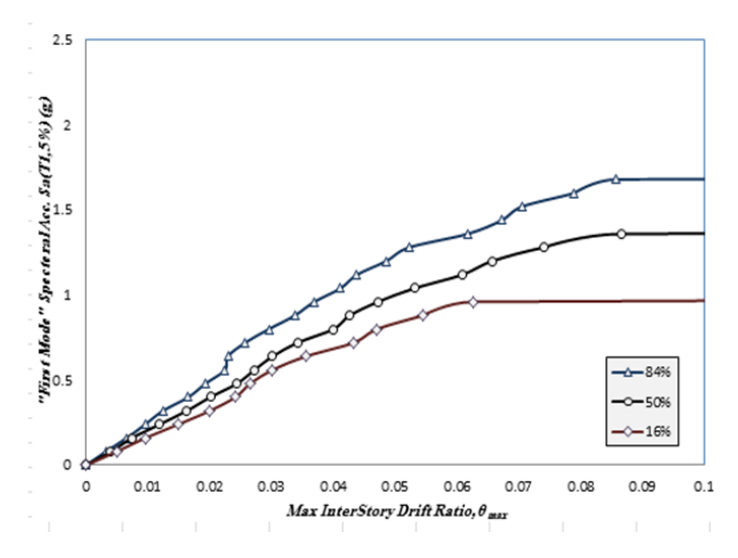


Fig. 15. 16%, 50%, and 84% percentile curves of the incremental nonlinear dynamic analysis for the 15-story structural frame (TYPE 2).

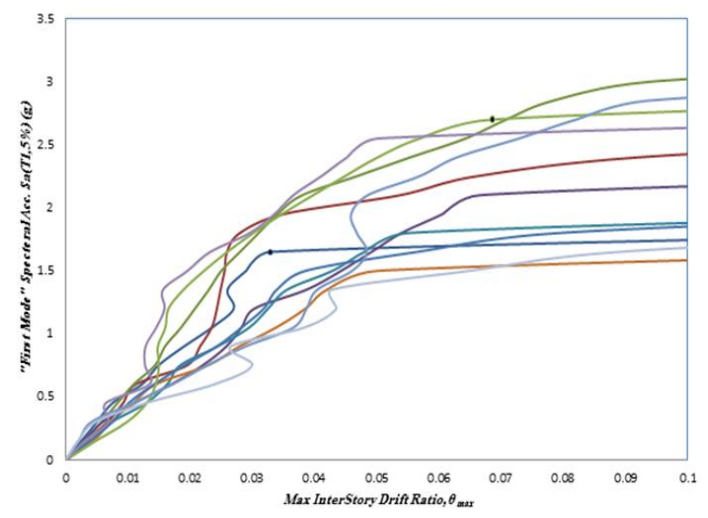


Fig 16. Incremental nonlinear dynamic curves obtained for the 15-story structural frame (TYPE 3).

Fig. 16 presents the incremental nonlinear dynamic curves for the 15-story structural frame of TYPE 3. Additionally, in Fig. 17, a summary of the IDA curves is shown, representing the 16%, 50%, and 84% percentiles.

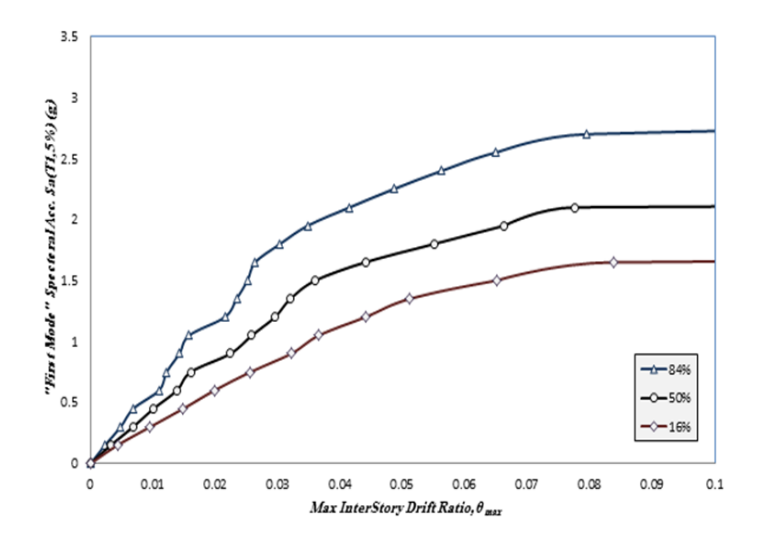


Fig.17. 16%, 50%, and 84% percentile curves of the incremental nonlinear dynamic analysis for the 15-story structural frame (TYPE 3).

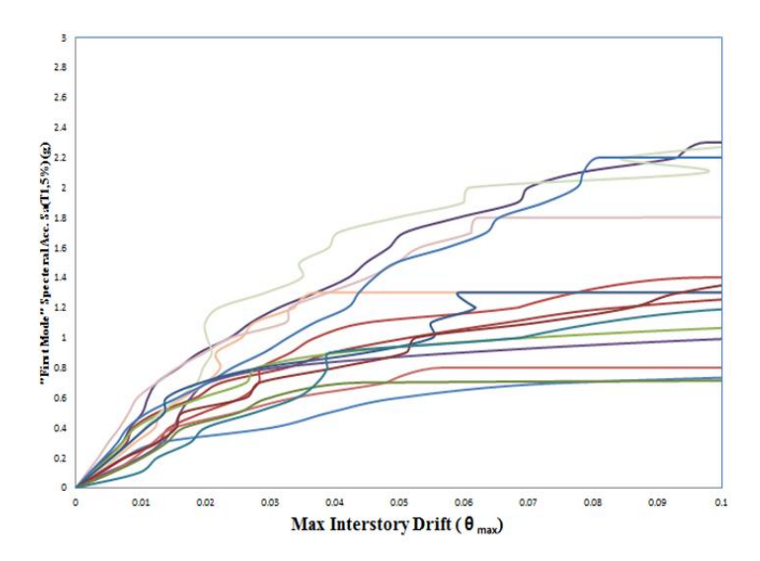


Fig. 18. Incremental nonlinear dynamic curves for the 15-story structural frame (TYPE 4).

Fig. 18 presents the incremental nonlinear dynamic curves for the 15-story structural frame of TYPE 4. Additionally, in Fig. 19, a summary of the IDA curves is shown, representing the 16%, 50%, and 84% percentiles.

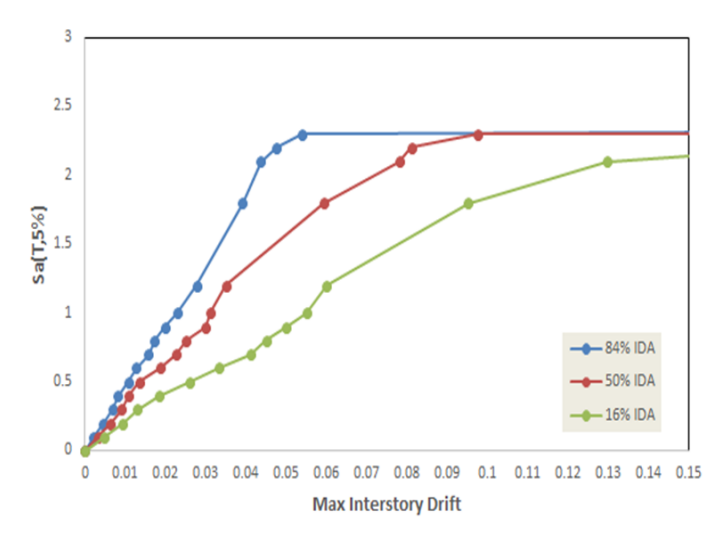


Fig. 19. 16%, 50%, and 84% percentile curves of the incremental nonlinear dynamic analysis for the 15-story structural frame (TYPE 4).

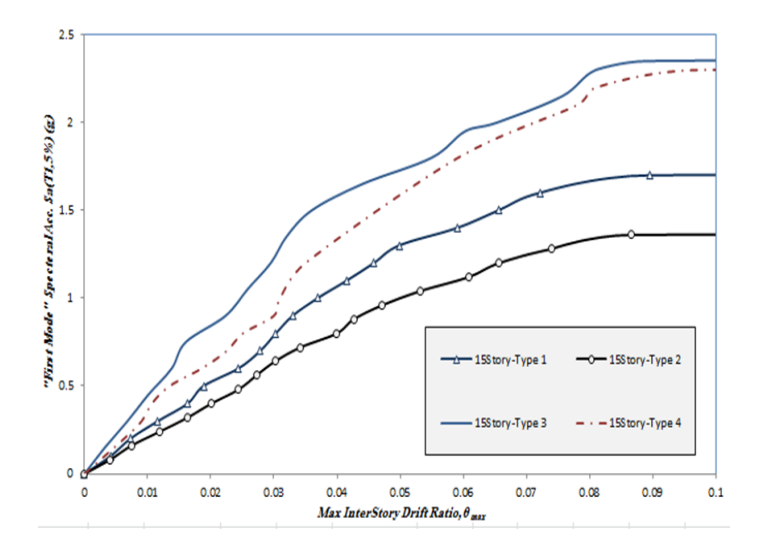


Fig. 20. Comparison of the 50% mean curves of the incremental nonlinear dynamic analysis for all four structural frames.

In Figs. 4-9, the 50% mean curves of the incremental nonlinear IDA for all four structural frames are presented. As observed, TYPE 3 exhibits higher stiffness, with its curve flattening at a higher level of seismic intensity. In contrast, TYPE 2 shows greater ductility, with its curve flattening at a lower level of seismic intensity.

## 5.2 | Derivation of Fragility Curves

As mentioned in this thesis, fragility curves are used to estimate the probability of reaching limit states based on the results of incremental nonlinear IDA. To plot these curves, the seismic intensity measure (IM) corresponding to the occurrence of the desired limit states is sorted in descending order for all ground motion records.

It should be noted that, according to FEMA 350 guidelines, the collapse limit state (CP) is defined as the point corresponding to 20% of the initial average slope, which represents the onset of flattening in the IDA curves.

The resulting fragility curves and their comparison are illustrated in Figure 21.

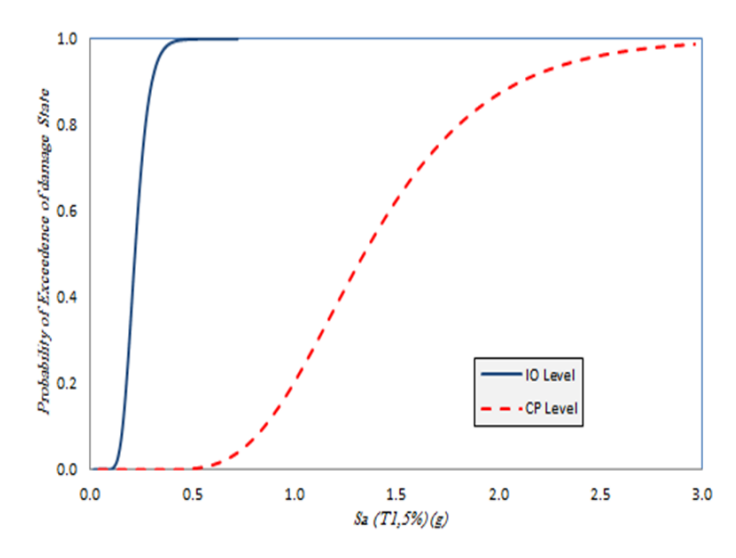


Fig. 21. Fragility curves derived from the incremental nonlinear dynamic analysis for the 15-story structural frame (TYPE 1) corresponding to the immediate occupancy and CP damage states.

In Fig. 21, the fragility curves derived from the incremental nonlinear IDA are presented for the 15-story structural frame of TYPE 1, corresponding to two damage states: Immediate Occupancy (IO) and Collapse Prevention (CP).

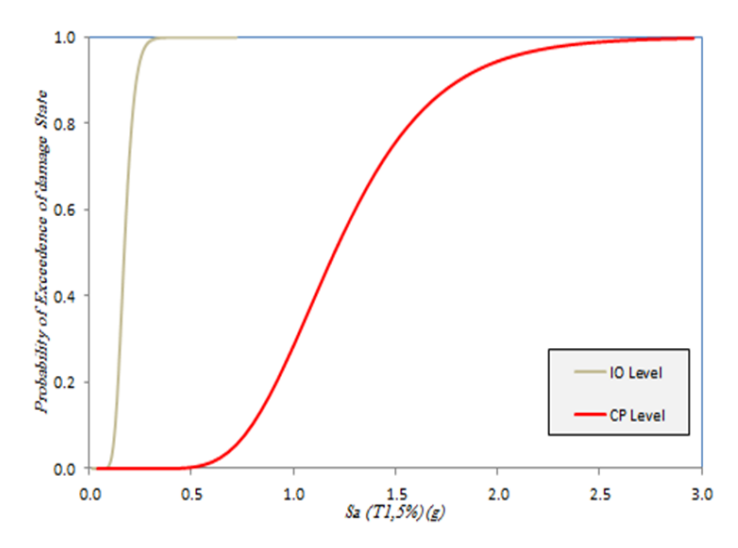


Fig. 22. Fragility curves derived from the incremental nonlinear dynamic analysis for the 15-story structural frame (TYPE 2) corresponding to the IO and CP damage states.

In Fig. 22, the fragility curves derived from the incremental nonlinear IDA are presented for the 15-story structural frame of TYPE 2, corresponding to two damage states: IO and CP.

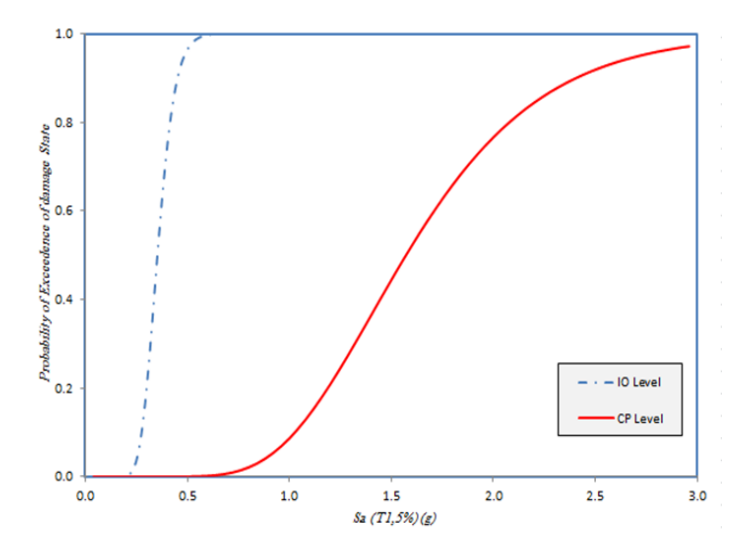


Fig. 23. Fragility curves derived from the incremental nonlinear dynamic analysis for the 15-story structural frame (TYPE 3) corresponding to the IO and CP damage states.

In Fig. 23, the fragility curves derived from the incremental nonlinear IDA are presented for the 15-story structural frame of TYPE 3, corresponding to two damage states: IO and CP.

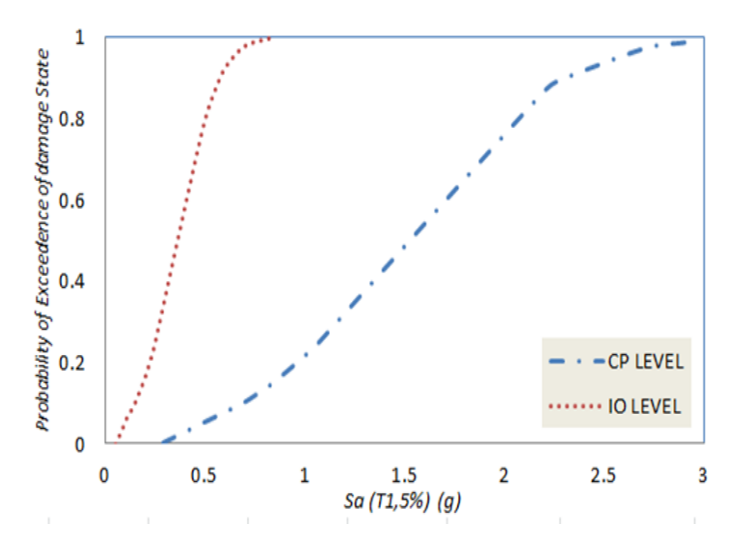


Fig. 24. Fragility curves derived from the incremental nonlinear dynamic analysis for the 15-story structural frame (TYPE 4) corresponding to the CP damage state.

In Fig. 24, the fragility curves derived from the incremental nonlinear IDA are presented for the 15-story structural frame of TYPE 4, corresponding to two damage states: IO and CP.

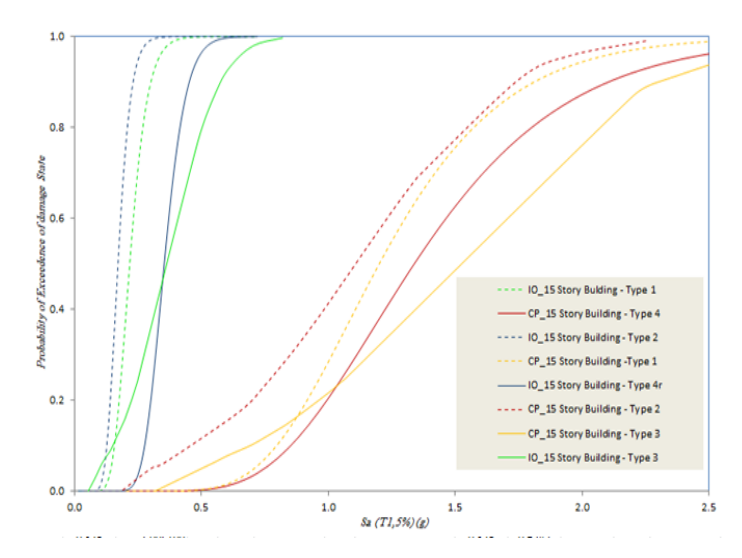


Fig. 25. Comparison of fragility curves derived from the incremental nonlinear dynamic analysis for the CP and IO damage states across all four structural frames.

In Figs. 4-14, a comparison of the fragility curves derived from the incremental nonlinear IDA is presented for the IO and CP damage states across all four structural frames. As observed, no clear trend is evident among the four structures.

## 6 | Conclusion

In this study, the behavior of structures equipped with optimized ADAS dampers in different configurations was thoroughly investigated. Such comprehensive research has rarely been conducted in the country, and given the growing trend toward this type of structural retrofitting, this project can be considered a novel and practical step in this field. The key findings of this research are summarized as follows:

- I. As observed, different damper configurations result in varying structural behaviors. Additionally, the type of dampers, considering their stiffness and performance, also affects the structural response. However, it cannot be conclusively stated which configuration provides the best performance, as the behaviors of all four configurations are very similar. The minor differences may be attributed to nonlinear analysis errors in the software. Nevertheless, all four configurations can be considered suitable retrofitting options, depending on the client's executive feasibility and requirements.
- II. The use of dampers in configurations 3 and 4 increases structural stiffness, reducing interstory drifts and minimizing both structural and non-structural damage.
- III. TADAS and ADAS dampers exhibit desirable seismic performance and can endure numerous loading cycles without a significant reduction in stiffness or strength.
- IV. Implementing dampers positively affects both global and local responses of the sample structures under seismic records, contributing effectively to structural strengthening and retrofitting.

## Acknowledgments

The authors would like to express their sincere gratitude to all colleagues and institutions that provided support and guidance during the course of this research.

## **Funding**

This research received no specific grant from any funding agency in the public, commercial, or not-for-profit sectors.

#### **Data Availability**

The data that support the findings of this study are available from the corresponding author upon reasonable request.

#### References

- [1] Stiemer, S. F., & Godden, W. G. (1980). Shaking table tests of piping systems with energy absorbing restrainers. University of California Earthquake Engineering Research Center. https://books.google.nl/books?redir\_esc=y&hl=nl&id=h0c4uE9SXywC&focus=searchwithinvolum
- [2] Bergman, D. M., & Goel, S. C. (1987). Evaluation of cyclic testing of steel-plate devices for added damping and stiffness. Department of Civil Engineering, University of Michigan. https://search.worldcat.org/es/title/evaluation-of-cyclic-testing-of-steel-plate-devices-for-addeddamping-and-stiffness/oclc/20751244
- [3] Tehranizadeh, M. (2001). Passive energy dissipation device for typical steel frame building in Iran. Engineering structures, 23(6), 643–655. https://doi.org/10.1016/S0141-0296(00)00082-1
- [4] Tsai, K. C., Chen, H. W., Hong, C. P., & Su, Y. F. (1993). Design of steel triangular plate energy absorbers for seismic-resistant construction. *Earthquake spectra*, *9*(3), 505–528. https://doi.org/10.1193/1.1585727
- [5] Moreschi, L. M. (2000). Seismic design of energy dissipation systems for optimal structural performance [Thesis]. https://www.proquest.com/openview/cce3cfa53baa8c00b4c3c0165bcf2a23/1?pq-origsite=gscholar&cbl=18750&diss=y
- [6] Xia, C., & Hanson, R. D. (1992). Influence of ADAS element parameters on building seismic response. Journal of structural engineering, 118(7), 1903–1918. https://doi.org/10.1061/(ASCE)0733-9445(1992)118:7(1903)
- [7] Workman, G. H. (1969). The inelastic behavior of multistory braced frame structures subjected toearthquake excitation. University of Michigan. https://www.proquest.com/openview/3b615370cadc4f9d0257073d883ccc60
- [8] Akkari, M. M. (1985). NONLINEAR dynamic analysis using mode superposition [thesis]. https://elibrary.ru/item.asp?id=7421113
- [9] Gholizadeh, S., Kamyab, R., Dadashi, H., & others. (2013). Performance-based design optimization of steel moment frames. *International journal of optimization in civil engineering*, 3(2), 327–343. https://www.sid.ir/fileserver/je/1037920130208.pdf
- [10] Moghaddam, H., Hajirasouliha, I., & Doostan, A. (2005). Optimum seismic design of concentrically braced steel frames: concepts and design procedures. *Journal of constructional steel research*, 61(2), 151–166. https://doi.org/10.1016/j.jcsr.2004.08.002
- [11] Farshidianfar, A., & Soheili, S. (2013). Ant colony optimization of tuned mass dampers for earthquake oscillations of high-rise structures including soil--structure interaction. *Soil dynamics and earthquake engineering*, 51, 14–22. https://doi.org/10.1016/j.soildyn.2013.04.002
- [12] Farshidianfar, A., & Soheili, S. (2013). Optimization of TMD parameters for earthquake vibrations of tall buildings including soil structure interaction. *International journal of optimization in civil engineering*, 3(3), 409–429. https://www.researchgate.net/publication/309762144\_Optimization\_of\_TMD\_parameters\_for
- [13] Nabid, N., Hajirasouliha, I., & Petkovski, M. (2019). Adaptive low computational cost optimisation method for Performance-based seismic design of friction dampers. *Engineering structures*, 198, 109549. https://doi.org/10.1016/j.engstruct.2019.109549
- [14] Zhang, S. Y., Jiang, J. Z., & Neild, S. A. (2017). Passive vibration control: a structure--immittance approach. *Proceedings of the royal society a: mathematical, physical and engineering sciences*, 473(2201), 20170011. https://doi.org/10.1098/rspa.2017.0011
- [15] Shojaeifar, H., Maleki, A., & Lotfollahi-Yaghin, M. A. (2020). Performance evaluation of curved-TADAS damper on seismic response of moment resisting steel frame. *Int. j. eng*, 33(1), 55–67. https://doi.org/10.5829/ije.2020.33.01a.07

- [16] Lv, Y., Li, L., Wu, D., Zhong, B., Chen, Y., & Chouw, N. (2019). Experimental Investigation of Steel Plate Shear Walls under Shear-Compression Interaction. *Shock and vibration*, 2019(1), 8202780. https://doi.org/10.1155/2019/8202780
- [17] Khoshkalam, M., Mortezagholi, M. H., & Zahrai, S. M. (2022). Proposed modification for ADAS damper to eliminate axial force and improve seismic performance. *Journal of earthquake engineering*, 26(10), 5130–5152. https://doi.org/10.1080/13632469.2020.1859419
- [18] De Domenico, D., & Ricciardi, G. (2018). Earthquake protection of existing structures with limited seismic joint: base isolation with supplemental damping versus rotational inertia. *Advances in civil engineering*, 2018(1), 6019495. https://doi.org/10.1155/2018/6019495
- [19] De Stefano, M., & Pintucchi, B. (2008). A review of research on seismic behaviour of irregular building structures since 2002. *Bulletin of earthquake engineering*, 6(2), 285-308. https://doi.org/10.1007/s10518-007-9052-3
- [20] Peruš, I., & Fajfar, P. (2002). On inelastic seismic response of an asymmetric single-storey structures under biaxial excitation. Third European Workshop on the Seismic Behaviour of Irregular and Complex Structures. https://www.caee.ca/8CCEEpdf/121 On Inelastic Seismic Response Of Asym
- [21] Kan, C. L., & Chopra, A. K. (1977). Effects of torsional coupling on earthquake forces in buildings. *Journal of the structural division*, 103(4), 805–819. https://doi.org/10.1061/JSDEAG.0004608
- [22] Irvine, H., & Kountouris, G. (1980). Peak ductility demands in simple torsionally unbalanced building models subjected to earthquake ground excitation. *Proceedings of 7th world conference on earthquake engineering*. https://www.iitk.ac.in/nicee/wcee/article/7\_vol4\_117.pdf?utm\_source=chatgpt.com